ARTICLES
https://doi.org/10.1038/s41564-022-01170-4
nature microbiology

Check for updates

Therapeutic efficacy of monoclonal antibodies and antivirals against SARS-CoV-2 Omicron BA.1 in Syrian hamsters

Ryuta Uraki[1,2,5], Maki Kiso[1,5], Masaki Imai[1,2,5], Seiya Yamayoshi[1,2], Mutsumi Ito[1], Seiichiro Fujisaki[3], Emi Takashita[3], Michiko Ujie[1,2], Yuri Furusawa[1,2], Atsuhiro Yasuhara[1], Kiyoko Iwatsuki-Horimoto[1], Yuko Sakai-Tagawa[1], Shinji Watanabe[3], Hideki Hasegawa[3] and Yoshihiro Kawaoka[1,2,4] ✉

The spike protein of severe acute respiratory syndrome coronavirus 2 (SARS-CoV-2) is the major antigen stimulating the host's protective immune response. Here we assessed the efficacy of therapeutic monoclonal antibodies (mAbs) against Omicron variant (B.1.1.529) sublineage BA.1 variants in Syrian hamsters. Of the FDA-approved therapeutic mAbs tested (that is, REGN10987/REGN10933, COV2-2196/COV2-2130 and S309), only COV2-2196/COV2-2130 efficiently inhibited BA.1 replication in the lungs of hamsters, and this effect was diminished against a BA.1.1 variant possessing the S-R346K substitution. In addition, treatment of BA.1-infected hamsters with molnupiravir (a SARS-CoV-2 RNA-dependent RNA polymerase inhibitor) or S-217622 (a SARS-CoV-2 protease inhibitor) strongly reduced virus replication in the lungs. These findings suggest that the use of therapeutic mAbs in Omicron-infected patients should be carefully considered due to mutations that affect efficacy, and demonstrate that the antiviral compounds molnupiravir and S-217622 are effective against Omicron BA.1 variants.

Severe acute respiratory syndrome coronavirus 2 (SARS-CoV-2), which is responsible for coronavirus disease 2019 (COVID-19), continues to spread around the world and has caused 6.1 million deaths so far. The Omicron variant (B.1.1.529) of SARS-CoV-2 was detected in November 2021 in South Africa and has spread rapidly around the world. Omicron variants have been classified into six different sublineages: BA.1, BA.1.1, BA.2, BA.3, BA.4 and BA.5. The original Omicron lineage, BA.1, rapidly became the prevailing variant circulating in many countries. A notable feature of the BA.1 variant is that it contains more than 30 amino acid substitutions in its spike (S) protein, which induces the immune responses of the host, specifically the production of neutralizing antibodies[1]. Importantly, 15 of these substitutions are in the receptor-binding domain (RBD) of the S protein, which is the major target for monoclonal antibody (mAb)-based therapy, raising concerns of decreased effectiveness of current therapeutic monoclonal antibodies (mAbs) for COVID-19 against this variant.

Recent studies using in vitro neutralization assays have demonstrated that the BA.1 variants show reduced sensitivity to some monoclonal and polyclonal antibodies relative to past isolates or other SARS-CoV-2 variants[2–6]. However, the in vivo efficacy of mAbs against the BA.1 variant is unknown. Here we assessed the efficacy of U.S. Food and Drug Administration (FDA)-approved therapeutic mAbs against BA.1 variants in Syrian hamsters, a well-established animal model for SARS-CoV-2 research[7–9]. In addition, using this model, we evaluated the therapeutic efficacy of small-molecule antiviral agents for COVID-19 against these variants.

Results

Therapeutic effects of mAbs on BA.1 variants. As of April 2022, the FDA has issued Emergency Use Authorizations (EUAs) to permit the emergency use of four different mAbs as therapeutic agents for the treatment and/or prevention of COVID-19 in adult and paediatric patients: REGEN-COV, a combination of imdevimab (REGN10987) and casirivimab (REGN10933); Xevudy, which is sotrovimab (VIR-7831); Evusheld (AZD7442), a combination of tixagevimab (COV2-2196 or AZD8955) and cilgavimab (COV2-2130 or AZD1061); and bebtelovimab (LY-CoV1404). We tested REGN10987/REGN10933, S309 (which is the precursor of sotrovimab) and COV2-2196/COV2-2130 for their therapeutic efficacy against BA.1. Sotrovimab for clinical use has been engineered with two amino acid mutations (M428L/N434S) in the fragment crystallizable (Fc) region, which extend the half-life of antibodies in vivo[10]. Both the COV2-2196 and COV2-2130 mAbs for clinical use contain the M252Y/S254T/T256E and L234F/L235E/P331S mutations in their Fc regions, which increase the half-life of antibodies and reduce the effector functions of antibodies, respectively[11–13]. All of the mAbs used in this study were synthesized according to publicly available sequences without any modifications (see Methods)[14]. The reactivity of all five mAbs was validated using enzyme-linked immunosorbent assay (ELISA) plates coated with recombinant S protein derived from the reference strain Wuhan/Hu-1/2019 and from a representative Omicron variant, and by neutralization assays; the results were consistent with previously published data[4,6,14]. We treated five hamsters with a single dose of the REGN10987/REGN10933 or

[1]Division of Virology, Institute of Medical Science, University of Tokyo, Tokyo, Japan. [2]The Research Center for Global Viral Diseases, National Center for Global Health and Medicine Research Institute, Tokyo, Japan. [3]Center for Influenza and Respiratory Virus Research, National Institute of Infectious Diseases, Musashimurayama, Tokyo, Japan. [4]Influenza Research Institute, Department of Pathobiological Sciences, School of Veterinary Medicine, University of Wisconsin-Madison, Madison, WI, USA. [5]These authors contributed equally: Ryuta Uraki, Maki Kiso, Masaki Imai. ✉e-mail: yoshihiro.kawaoka@wisc.edu

COV2-2196/COV2-2130 combination (2.5 mg kg^{-1} each), or S309 as monotherapy (5 mg kg^{-1}) by intraperitoneal injection on Day 1 after intranasal inoculation with 10^3 plaque-forming units (p.f.u.) of CoV-2/UT-HP095-1N/Human/2020/Tokyo (D614G; HP095) or hCoV-19/Japan/NC928-2N/2021 (Omicron BA.1; NC928) (Fig. 1a). A human mAb specific to the haemagglutinin of influenza B virus was injected intraperitoneally to five hamsters on Day 1 post-infection as a control. The animals were killed, and nasal turbinate and lung samples were collected for virus titrations on Day 4 post-infection. Sera were also collected at this timepoint and tested in an ELISA for RBD-specific IgG antibodies to confirm successful antibody transfer. Hamsters with low levels of ELISA titre (≤640) were excluded from further analysis.

For the D614G (HP095)-infected groups, treatment with REGN10987/REGN10933 or COV2-2196/COV2-2130 resulted in a significant reduction in virus titres in both the nasal turbinates (mean reduction in viral titre, 2.9 and 3.2 $\log_{10}$(p.f.u. g^{-1}), respectively) and lungs (mean reduction in viral titre, 2.9 and 2.4 $\log_{10}$(p.f.u. g^{-1}), respectively) compared with control mAb-treated animals (Fig. 1b). These results are consistent with those of previous studies in which the combinations of REGN10987/REGN10933 or COV2-2196/COV2-2130 were shown to have therapeutic activity against infection with early (USA-WA1/2020) or variant (USA-WA1/2020 N501Y/D614G) SARS-CoV-2 strains in rhesus macaques, hamsters and mice[15–17]. Virus titres in the lungs of animals treated with S309 were significantly lower than those in the organs of animals treated with the control mAb (mean reduction in viral titre, 1.5 $\log_{10}$ (p.f.u. g^{-1})). In contrast, no differences in viral titres in the nasal turbinates were observed between the animals that were treated with this mAb and those treated with the control mAb. Thus, S309 showed less therapeutic effect against infection with D614G (HP095) compared with the other mAbs. For the BA.1 (NC928)-infected groups, neither S309 nor REGN10987/REGN10933 influenced the virus titres in the nasal turbinates or the lungs of the animals (Fig. 1c). However, COV2-2196/COV2-2130 significantly reduced the virus titres in the lungs of the animals (mean reduction in viral titre, 2.7 $\log_{10}$(p.f.u. g^{-1})), whereas the virus titres in their nasal turbinates were not affected by this treatment. Previous studies have shown that mutations at amino acid position 346 of the RBD affect the binding of class 3 mAbs such as COV2-2130[18–21]. Next, we examined the neutralization activities of mAbs against an Omicron BA.1.1 (that is, hCoV-19/Japan/NC929-1N/2021; NC929; BA.1.1 is a subvariant of BA.1 possessing the R346K mutation in the S protein). A live-virus focus reduction neutralization assay revealed that BA.1.1 was neutralized by S309, REGN10933, COV2-2196, COV2-2130 or the combination of COV2-2196 and COV2-2130 to varying degrees (Supplementary Table 1), similar to our previous findings with Omicron BA.1 (NC928)[14]. However, unlike our previous results with BA.1 (NC928), COV2-2130 showed extremely high 50% focus reduction neutralization titre ($FRNT_{50}$) values against BA.1.1 (NC929, 13,558.20 ng ml^{-1}), suggesting that this therapeutic mAb may not be effective against BA.1.1 variants encoding the S-R346K mutation. We therefore asked whether the COV2-2196/COV2-2130 combination or COV2-2130 as monotherapy could inhibit the replication of BA.1.1 (NC929) in the respiratory tract of hamsters. We found that neither COV2-2130 nor COV2-2196/COV2-2130 had an effect on the virus titres in the nasal turbinates or the lungs of the animals (Fig. 1d). Taken together, these results indicate that the COV2-2196/COV2-2130 combination can restrict viral replication in the lungs of animals infected with BA.1 bearing S-346R even if the mAbs are administrated after the infection has occurred. In contrast, the COV2-2196/COV2-2130 combination may not be effective against BA.1.1 harbouring the S-R346K mutation.

Therapeutic effects of antivirals on BA.1 variants. Molnupiravir (an inhibitor of the RNA-dependent RNA polymerase of SARS-CoV-2) was approved by the FDA for the treatment of adult patients with COVID-19 on 23 December 2021. S-217622, an inhibitor of the main protease (also called 3CLpro) of SARS-CoV-2, is currently in clinical trials. We previously showed that the susceptibility of BA.1 (NC928) to molnupiravir was comparable to that of an early SARS-CoV-2 strain (NC002) and other variants of concern[14]. In this study, we confirmed that the BA.1 variant and the early (SARS-CoV-2/UT-NC002-1T/Human/2020/Tokyo) strains have similar sensitivities to S-217622 in vitro (Supplementary Table 2).

After establishing the in vitro sensitivity of the BA.1 variants to antiviral compounds, we assessed their therapeutic efficiencies in hamsters infected with the BA.1 (NC928). The dosage of molnupiravir for hamsters was determined on the basis of previous studies to evaluate the effect of molnupiravir against SARS-CoV-2 in the mouse model[22]. For S-217622, first we evaluated its pharmacokinetic (PK) parameters in hamsters. In hamsters administered S-217622 at 60 mg kg^{-1}, the plasma concentration of S-217622 reached the maximum at 1.88 h and then declined with a half-life ($t_{1/2,z}$) value of 3.43 h. The maximum concentration (C_{max}), area under the concentration–time curve $(AUC)_{0-24h}$ and $AUC_{0\text{-}inf}$ values at 60 mg kg^{-1} were 128 μM, 937 μM h and 945 μM h, respectively (Extended Data Fig. 1 and Supplementary Table 3). These PK parameters indicate that the plasma concentration of S-217622 would be expected to be 15.6 μM at 12 h after dosing at 60 mg kg^{-1}, which is higher than the 50% effective concentration (EC_{50}; 1.73 μM) (Supplementary Table 2); therefore, we determined that we would administer S-217622 at a dosage of 60 mg kg^{-1} per 12 h. Hamsters intranasally infected with 10^3 p.f.u. of virus were treated by oral gavage twice daily (at 12 h intervals) for 1, 2 or 3 d with 500 mg kg^{-1} per 12 h (1,000 mg kg^{-1} d^{-1}) molnupiravir or with 60 mg kg^{-1} per 12 h (120 mg kg^{-1} d^{-1}) S-217622, beginning at 24 h post-infection (Fig. 2a). On Days 2, 3 or 4 post-infection, the animals were killed, and nasal turbinates and lungs were collected for virus titration. Although no differences in the virus titres in the nasal turbinates were found between the animals that were treated with molnupiravir and those treated with methylcellulose (control) on Days 3 and 4 post-infection, treatment with this compound led to a significant 7.3-fold reduction in virus titres in the nasal turbinates on Day 2 post-infection (Fig. 2b). Treatment with S-217622 resulted in significant 18.3 and 9.9-fold reductions in virus titres in the nasal turbinates on Days 2 and 4 post-infection, respectively. Moreover, both compounds dramatically reduced lung virus titres; no virus was recovered from the lungs of all four animals treated with molnupiravir at any timepoint post-infection, from the lungs of all four animals treated with S-217622 on Days 2 and 3 post-infection, or from the lungs of 3 of the 4 animals treated with S-217622 on Day 4 post-infection.

Prolonged replication of influenza viruses in drug recipients is associated with an increased risk of emergence of antiviral drug resistance[23–25]. Therefore, we asked whether treatment with these compounds in immunosuppressed hosts with prolonged viral shedding could result in the emergence of resistant variants. To generate an immunocompromised model, cyclophosphamide (CPA) was administered intraperitoneally to hamsters on Days −3, 1, 5 and 9 relative to infection as described previously[26] (Fig. 2c). On Day 7 post-infection, virus titres were low in the nasal turbinates and lungs of untreated hamsters (Fig. 2d). In contrast, high levels of infection were sustained in the respiratory tract of the CPA-treated animals on Days 7 and 14 post-infection, indicating that immunosuppressive treatment with CPA lead to prolonged viral shedding. Both molnupiravir and S-217622 efficiently inhibited virus replication in the lungs of the immunosuppressed animals on Day 7 post-infection (mean reduction in viral titre, 4.2 and 3.4 $\log_{10}$(p.f.u. g^{-1}), respectively) (Fig. 2d). These compounds also reduced the levels of infectious virus in the lungs on Day 14 post-infection, although the difference compared with the vehicle control group was not statistically significant. However,

a

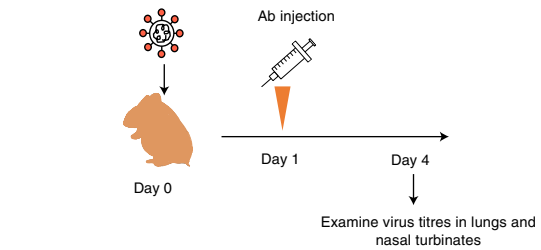

Virus	Infection route	Infection titre
D614G (HP095)	Intranasal	10^3 p.f.u./30 µl
Omicron/BA.1 (NC928)	Intranasal	10^3 p.f.u./30 µl
Omicron/BA1.1 (NC929)	Intranasal	10^3 p.f.u./30 µl

Antibody	Inoculation route	Concentration (mg kg^{-1})
S309	Intraperitoneal	5
REGN10987 REGN10933	Intraperitoneal	2.5 2.5
COV2-2196 COV2-2130	Intraperitoneal	2.5 2.5
Control (1430E3/9)	Intraperitoneal	5

b D614G (HP095)

Treatment antibody	Animal ID #	Antibody endpoint titre	Virus titres ($\log_{10}$ p.f.u. g^{-1}) Lung	Nasal turbinate
S309	1	160	8.22	6.75
	2	20,480	7.03	6.66
	3	40,960	6.78	7.27
	4	20,480	7.05	6.61
	5	40,960	6.60	6.62
REGN10987 REGN10933	6	160	8.14	7.76
	7	81,920	5.61	5.51
	8	81,920	4.22	3.17
	9	81,920	5.80	4.96
	10	81,920	6.09	2.99
COV2-2196 COV2-2130	11	40,960	6.31	4.36
	12	40,960	5.78	4.77
	13	81,920	6.76	2.73
	14	81,920	5.26	5.21
	15	81,920	5.80	2.24
Control mAb	16	<40	8.37	6.90
	17	<40	8.22	8.27
	18	<40	8.44	7.00
	19	<40	8.27	6.46
	20	<40	8.43	6.54

c Omicron/BA.1 (NC928)

Treatment antibody	Animal ID #	Antibody endpoint titre	Virus titres ($\log_{10}$ p.f.u. g^{-1}) Lung	Nasal turbinate
S309	21	1,280	5.84	6.49
	22	20,480	3.71	6.17
	23	20,480	6.34	6.12
	24	20,480	6.48	6.61
	25	40,960	6.45	6.79
REGN10987 REGN10933	26	40,960	6.97	8.06
	27	81,920	5.72	7.53
	28	81,920	4.32	6.65
	29	2,560	6.02	6.84
	30	81,920	6.22	7.07
COV2-2196 COV2-2130	31	81,920	3.96	5.71
	32	81,920	1.50	5.96
	33	81,920	3.86	6.90
	34	40,960	4.94	6.50
	35	20,480	5.05	7.55
Control mAb	36	<40	7.00	7.25
	37	<40	6.95	7.94
	38	<40	6.23	6.53
	39	<40	6.32	7.29
	40	<40	6.36	6.91

d Omicron/BA1.1 (NC929)

Treatment antibody	Animal ID #	Antibody endpoint titre	Virus titres ($\log_{10}$ p.f.u. g^{-1}) Lung	Nasal turbinate
COV2-2130	41	40,960	3.19	5.86
	42	20,480	6.11	6.72
	43	20,480	4.19	6.50
	44	40,960	3.77	6.74
	45	20,480	7.47	7.15
COV2-2196 COV2-2130	46	5,120	6.56	7.24
	47	40,960	5.86	6.68
	48	<40	5.99	6.26
	49	40	4.98	7.03
	50	40,960	3.08	5.84
Control mAb	51	<40	3.97	5.92
	52	<40	4.90	6.59
	53	<40	6.00	6.50
	54	<40	5.80	6.71
	55	<40	4.25	7.33

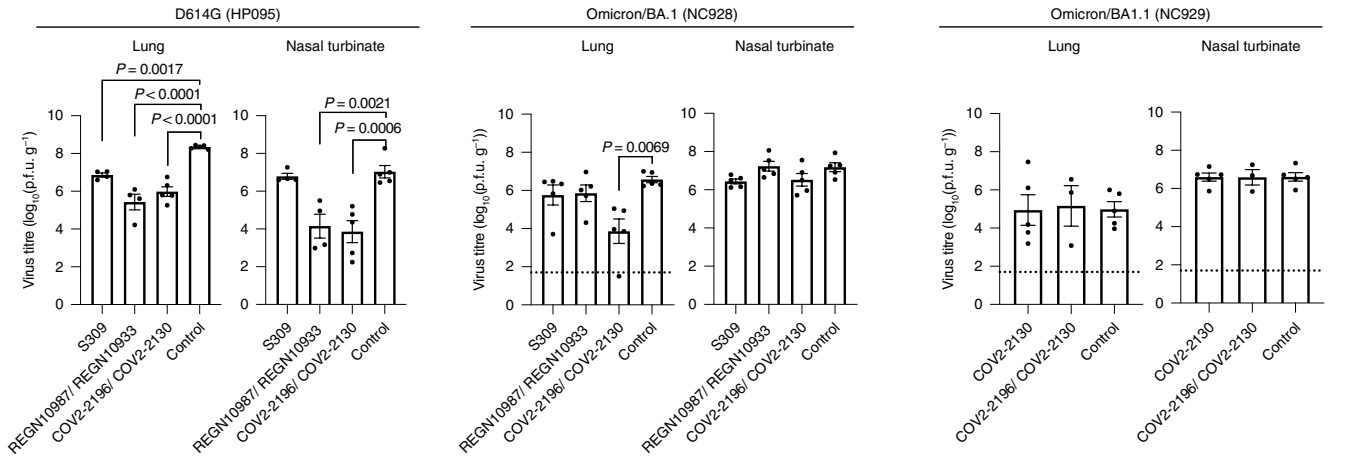

Fig. 1 | Therapeutic effects of monoclonal antibodies on the replication of SARS-CoV-2 Omicron BA.1 and BA.1.1 variants. a, Schematic diagram of the experimental workflow for assessing the therapeutic effects of monoclonal antibodies. **b**–**d**, Syrian hamsters were intranasally inoculated with 10^3 p.f.u. of D614G (HP095) (**b**), BA.1 (NC928) (**c**) or BA.1.1 (NC929) (**d**). On Day 1 post-infection of D614G (HP095) or BA.1 (NC928), the hamsters were intraperitoneally injected with a single dose of the REGN10987/REGN10933 or COV2-2196/COV2-2130 combination (2.5 mg kg^{-1} each), or S309 as monotherapy (5 mg kg^{-1}). On Day 1 post-infection with BA.1.1 (NC929), the hamsters were intraperitoneally injected with a single dose of COV2-2130 as monotherapy (5 mg kg^{-1}) or with the COV2-2196/COV2-2130 combination (2.5 mg kg^{-1} each). As a control, a human monoclonal antibody (1430E3/9) against the haemagglutinin of influenza B virus was injected. Hamsters were euthanized on Day 4 post-infection for virus titration. Sera were also collected at this timepoint, and titres of RBD-specific IgG antibodies in the sera were determined using ELISA plates coated with recombinant RBD derived from the S protein of Wuhan/Hu-1/2019 (GenBank accession no. MN908947). Top panels; ELISA titres and virus titres in animals treated with monoclonal antibodies. Red to blue shading represents the degree (high to low) of each titre in the animals. Bottom panels; bar graphs of virus titres in the respiratory organs of animals whose antibodies were successfully transferred. The endpoint titre is defined as the reciprocal of the highest dilution with an OD_{450} cut-off value ≥0.1. Antibody-transferred hamsters with low ELISA titres (≤640) (Nos. 1, 6, 48, and 49 denoted in red) were excluded from this analysis. The detection limit for virus titres was 1.7 $\log_{10}$(p.f.u. g^{-1}). Vertical bars show the mean ± s.e.m. Points indicate data from individual hamsters (**b**, S309 and REGN10987/REGN10933, $n = 4$; **d**, COV2-2196/COV2-2130, $n = 3$; other groups in **b**–**d**, $n = 5$). The lower limit of detection is indicated by the horizontal dotted line. To compare the lung titres of the different groups in the BA.1 (NC928)-infected hamsters, we used a Kruskal-Wallis test followed by Dunn's multiple comparisons test. To compare the nasal turbinate and lung titres of the different groups in the D614G (HP095) or BA.1.1 (NC929)-infected hamsters and the nasal turbinate titres of the different groups in the BA.1 (NC928)-infected hamsters, we used a one-way ANOVA followed by Dunnett's multiple comparisons test. $P < 0.05$ was considered statistically significant.

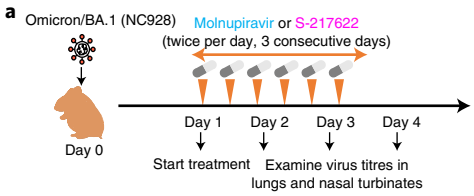

Virus	Infection route	Infection titres
Omicron/BA.1 (NC928)	Intranasal	10^3 p.f.u./30 µl

Antivirals	Inoculation route	Concentration (mg kg^{-1})	Inoculation (hpi)
Molnupiravir	Oral	500	24, 36, 48, 60, 72 and 84
S-217622	Oral	60	

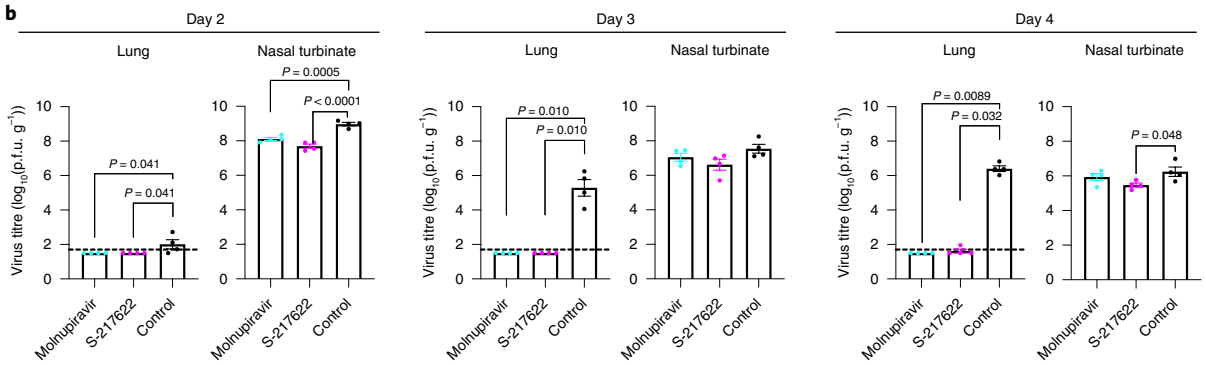

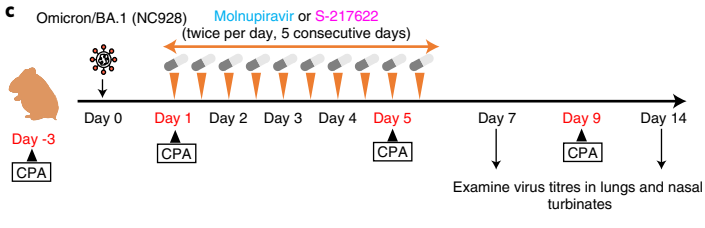

Virus	Infection route	Infection titres
Omicron/BA.1 (NC928)	Intranasal	10^3p.f.u./30 µl

Antiviral	Inoculation route	Concentration (mg kg^{-1})	Inoculation (hpi)
Molnupiravir	Oral	500	24, 36, 48, 60, 72, 84, 96, 108, 120, and 132
S-217622	Oral	60	

Compound for immunosuppression	Inoculation route	Concentration and timing
Cyclophosphamide (CPA)	Intraperitoneal	140 mg kg^{-1} (Day −3), 100 mg kg^{-1} (Days 1, 5, and 9)

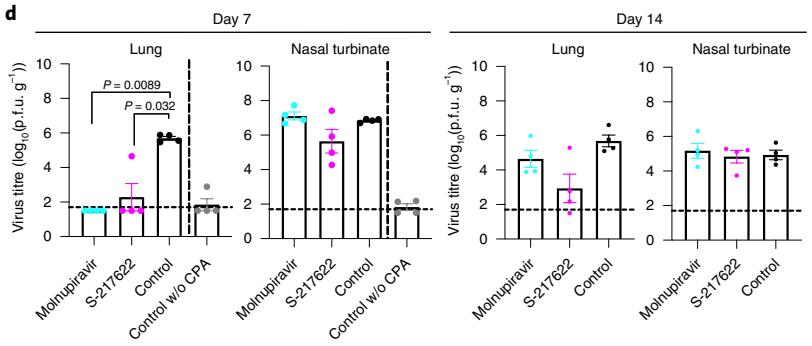

e

Sample collection timepoint:	Treatment compound	Animal ID #	Lung virus titres (log_{10} p.f.u. g^{-1})	Drug susceptibility of viruses isolated from lungs EIDD-1931 EC_{50} (µM)	Drug susceptibility of viruses isolated from lungs S-217622 EC_{50} (µM)
Day 7	Control	1	5.87	5.5	0.6
		2	5.56	5.5	0.6
		3	5.47	5.5	0.6
		4	5.89	5.5	0.6
	Molnupiravir	5	1.50	-	-
		6	1.50	-	-
		7	1.50	-	-
		8	1.50	-	-
	S-217622	9	1.50	-	-
		10	4.65	-	0.6
		11	1.50	-	-
		12	1.50	-	-
Day 14	Control	13	6.61	3.0	0.6
		14	5.10	2.1	0.6
		15	5.77	5.5	0.6
		16	5.27	5.5	0.2
	Molnupiravir	17	3.93	3.0	-
		18	5.98	5.5	-
		19	3.88	5.5	-
		20	4.80	3.0	-
	S-217622	21	2.17	-	0.3
		22	2.78	-	0.4
		23	5.29	-	0.3
		24	1.50	-	-

Fig. 2 | Therapeutic effects of antiviral compounds on the replication of the SARS-CoV-2 Omicron BA.1 variant. a, Schematic diagram of the experimental workflow for assessing the therapeutic effects of antiviral compounds. **b**, Syrian hamsters were intranasally inoculated with 10^3 p.f.u. of BA.1 (NC928). At 24 h post-infection (hpi), hamsters were treated with 500 mg kg^{-1} molnupiravir orally twice daily for 3 d or 60 mg kg^{-1} S-217622 orally twice daily for 3 d. Methylcellulose served as a control for oral treatment. Hamsters were euthanized on Days 2, 3 and 4 post-infection for virus titration. Vertical bars show the mean ± s.e.m. Points indicate data from individual hamsters ($n = 4$ per group). **c**, Schematic diagram of the experimental workflow for investigating the emergence of resistant variants. **d**,**e**, Four Syrian hamsters were intranasally inoculated with 10^3 p.f.u. of BA.1 (NC928). CPA was administered intraperitoneally to hamsters on Days −3, 1, 5 and 9 relative to infection. At 24 hpi, hamsters were treated with 500 mg kg^{-1} molnupiravir orally twice daily for 5 d or 60 mg kg^{-1} S-217622 orally twice daily for 5 d. Methylcellulose served as a control for oral treatment. **d**, Hamsters were euthanized on Days 7 and 14 post-infection for virus titration. Vertical bars show the mean ± s.e.m. Points indicate data from individual hamsters ($n = 4$ per group). **e**, Drug susceptibility of viruses. Viruses were isolated from the lungs of immunosuppressed animals treated with molnupiravir, S-217622 or the vehicle control on Days 7 and 14 post-infection. EC_{50} values of molnupiravir or S-217622 were determined using the Spearman–Karber formula on the basis of the appearance of visually detectable CPE in quadruplicate experiments. EIDD-1931 is the active form of molnupiravir. -, not applicable. Red to blue shading represents the degree (high to low) of each titre in the animals. In **b** and **d**, the lower limit of detection is indicated by horizontal dashed lines. To compare the lung and nasal turbinate titres of the different groups in the BA.1 (NC928)-infected hamsters, we used a Kruskal–Wallis test followed by Dunn's multiple comparisons test, and a one-way ANOVA followed by Dunnett's multiple comparisons test, respectively. $P < 0.05$ was considered statistically significant.

neither molnupiravir nor S-217622 affected the virus titres in the nasal turbinates of the animals on Days 7 and 14 post-infection. These results suggest that viral clearance cannot be achieved in immunocompromised hosts by the short-term use of these antiviral compounds. We determined the in vitro EC_{50} of molnupiravir and S-217622 against viruses isolated from the lungs of immunosuppressed animals treated with each compound or the vehicle control on Days 7 and 14 post-infection. The susceptibilities of isolates recovered from the drug-treated animals to each compound were comparable to those from control vehicle-treated animals (Fig. 2e). Deep sequencing analysis revealed that viruses isolated from the lungs of the molnupiravir-treated animal (#19) on Day 14 post-infection did not possess any mutations in the RNA-dependent RNA polymerase compared with the sequence from the samples from the control animal (#15) (Supplementary Table 4). No mutation was detected in the main protease of viruses recovered from the lungs of the S-217622-treated animals (#10 and #22) on Day 7 or Day 14 post-infection. The number of mutations detected in viruses isolated from the lungs of the molnupiravir-treated animal (#19) was greater than that from the control animal (#15) or S-217622-treated animals (#10 and #22). This finding is consistent with the mechanism of action of molnupiravir being a mutagen, leading to 'error catastrophe' during viral replication[27]. Together, these observations suggest that under the conditions tested, the emergence of resistant variants in immunosuppressed hamsters treated with molnupiravir or S-217622 appears to be limited.

Collectively, our observations suggest that the two antiviral compounds tested here considerably restrict Omicron BA.1 variant replication in the lower respiratory tract. In addition, animals treated with S-217622 had a significant reduction in virus titres in their upper respiratory tract.

Discussion

The emergence of SARS-CoV-2 Omicron variants carrying a large number of mutations in the RBD of the S protein has raised concern that these variants may limit the therapeutic usefulness of mAbs. In this study, we observed that the mAb combination COV2-2196/COV2-2130 efficiently suppressed the replication of an Omicron BA.1 variant lacking the S-R346K mutation in the lungs of hamsters when these mAbs were administrated 1 d post-infection, but was not effective against an Omicron BA.1.1 variant with the S-R346K mutation. Our results are consistent with those of previous studies in which mutations at position 346 of the RBD were found to confer immune escape from class 3 neutralizing mAbs such as COV2-2130[18–20].

Recent studies using in vitro neutralization assays have shown that sotrovimab and its parental form (S309) neutralize the Omicron variants[4,6,14]. In addition, prophylactic administration of hamster IgG2a S309 has been shown to prevent or significantly diminish the replication of SARS-CoV-2 in hamsters[28]. However, in this study, we observed that the therapeutic administration of this mAb had no effect on the virus titres in the respiratory tracts of hamsters infected with the BA.1 (NC928) variant. This lack of therapeutic efficacy against the BA.1 (NC928) variant may be due to the lower antibody-binding activities detected in animals at the time of virus titration (3 d after antibody administration) in S309-treated animals compared with COV2-2196/COV2-2130-treated animals (Fig. 1). Another study has shown that Fc effector functions enhance the therapeutic activity of neutralizing mAbs against SARS-CoV-2 infections in hamsters[29]. Because the S309 tested in this study originated from a human, its Fc receptor might not be optimal to recruit effector functions in hamsters. Further investigations are required to determine whether the replication of the BA.1 variants is efficiently inhibited by S309 possessing Fc domains modified to match the target host Fc receptors.

We observed that Omicron BA.1 variants replicated less efficiently in the lungs of infected hamsters (Fig. 2b), consistent with our previous study[30]. A recent study has shown that Omicron variants replicate to lower titres than Delta variants in lower airway organoids and Calu-3 lung cells[31], although Omicron and Delta variants replicate with similar efficiency in human nasal epithelial cultures. Human protein transmembrane protease serine 2 (TMPRSS2)[31], which is expressed at high levels in human and hamster lung[32,33], activates the S protein of SARS-CoV-2 and the S protein of Omicron variants has been shown to inefficiently use TMPRSS2. Therefore, the reduced TMPRSS2 usage of the Omicron S protein may affect the replication of Omicron variants in the lungs of humans and hamsters.

Our study has several potential limitations: (1) Although hamsters are one of the most susceptible animals to SARS-CoV-2 among those tested, including mice and non-human primates, the Omicron BA.1 variants are attenuated in hamsters especially in the lungs. It is not known whether the Omicron variants in humans are as attenuated as in hamsters. The difference (if any) in the replication of the Omicron variants in humans and hamsters may affect the effectiveness of the mAbs and antiviral compounds; (2) We did not see efficacy with some of the mAbs or mAb cocktails. Because it is difficult to administer a large volume of antibodies intravenously to hamsters, we administered them intraperitonially. However, in humans, they are administered intravenously. The route of administration may affect the efficacy of antibodies; (3) The mAbs generated in this study are not identical to the mAbs in clinical use because amino acid substitutions have been introduced into clinical mAbs to enhance their half-lives and reduce their effector functions and this difference may have led to the lower efficacy in the hamster model; and (4) The mAbs tested in this study have the human IgG1 Fc region. Because the Fcγ receptors of humans and hamsters are different, inefficient Fc-mediated effector functions elicited by interactions with Fcγ receptors may have affected the efficacy in hamsters.

In conclusion, our data show that the two small-molecule antiviral agents molnupiravir and S-217622 may have therapeutic value against Omicron BA.1 variants of SARS-CoV-2. Our data also suggest that the mAb combination COV2-2196/COV2-2130 may be an effective treatment option against Omicron BA.1 variants that lack the S-R346K mutation. Importantly, however, this mAb combination may not provide effective treatment against Omicron BA.1.1 variants harbouring the S-R346K mutation. The use of therapeutic mAbs in patients infected with Omicron variants should be carefully considered.

Methods

Cells. VeroE6/TMPRSS2 (JCRB 1819) cells[34,35] were propagated in the presence of 1 mg ml^{-1} geneticin (G418; Invivogen) and 5 μg ml^{-1} plasmocin prophylactic (Invivogen) in Dulbecco's modified Eagle's medium (DMEM) containing 10% fetal calf serum and antibiotics, and maintained at 37 °C with 5% CO_2. Chinese hamster ovary (CHO) cells were maintained in DMEM containing 10% fetal calf serum and antibiotics at 37 °C with 5% CO_2. Expi293 cells (Thermo Fisher) were maintained in Expi293 expression medium (Thermo Fisher) at 37 °C under 8% CO_2. The cells were regularly tested for mycoplasma contamination using PCR, and confirmed to be mycoplasma-free.

Viruses. hCoV-19/Japan/NC928-2N/2021 (Omicron BA.1; NC928)[14], hCoV-19/Japan/NC929-1N/2021(Omicron BA.1.1; NC929), SARS-CoV-2/UT-NC002-1T/Human/2020/Tokyo (NC002)[7] and SARS-CoV-2/UT-HP095-1N/Human/2020/Tokyo (D614G; HP095)[35] were propagated in VeroE6/TMPRSS2 cells in VP-SFM (Thermo Fisher). All experiments with SARS-CoV-2 were performed in enhanced biosafety level 3 containment laboratories at the University of Tokyo, which are approved for such use by the Ministry of Agriculture, Forestry and Fisheries, Japan.

Antibodies. Amino acid sequences for the variable region of the heavy and light chains of the following human monoclonal antibodies against the S protein were used for gene synthesis: clones tixagevimab (COV2-2196/AZD8895; GenBank accession numbers QLI33947 and QLI33948), casirivimab (REGN10933; PDB accession numbers 6XDG_B and 6XDG_D), cilgavimab (COV2-2130/

AZD1061; GenBank accession numbers QKY76296 and QKY75909), imdevimab (REGN10987; PDB accession numbers 6XDG_A and 6XDG_A) and S309 (PDB accession numbers 6WS6_A and 6WS6_F). An artificial signal sequence and the constant gamma heavy (IgG1, UniProtKB/Swiss-Prot accession number P01857) and kappa (UniProtKB/Swiss-Prot accession number P01834) or lambda (UniProtKB/Swiss-Prot accession number P0DOY2) light chain coding sequences were added before and after each variable region. Codon usage was optimized for expression in CHO cells. The synthesized genes were cloned into a plasmid for protein expression and transfected into CHO cells. Cell culture media were collected after incubation for 10–14 d at 37 °C. A human monoclonal antibody (1430E3/9) against the haemagglutinin of influenza B virus[36] was previously cloned into the expression vector Mammalian Power Express System (TOYOBO) and was transiently expressed by Expi293 cells. Monoclonal antibodies were purified by using MabSelect SuRe LX (Cytiva) or a protein A column. Purity was confirmed by SDS–PAGE and/or HPLC before use. The reactivities of these antibodies against SARS-CoV-2, including the Alpha, Beta, Delta, Gamma and Omicron variants, have been tested previously[14].

Antiviral compounds. Molnupiravir (EIDD-2801) was purchased from MedChemExpress. S-217622 was kindly provided by Shionogi Co., Ltd. All compounds were dissolved in 0.5% methylcellulose before use in in vivo experiments.

Pharmacokinetics studies in Syrian hamsters. Male Syrian hamsters (5 weeks) were purchased from Japan SLC. The dosing vehicle was 0.5% (w/v) methylcellulose (400 cP). The compound was orally administered at 60 mg kg^{-1} ($n = 4$) under non-fasted conditions. Blood samples (0.1 ml) were collected with disposable syringes containing anticoagulants (EDTA 2K and heparin) at 0.5, 1, 2, 4, 8 and 24 h after dosing. Blood samples were centrifuged (1,800 × g, 4 °C, 10 min) to obtain plasma samples, which were transferred to tubes and stored in a freezer until analysed. Plasma concentrations were determined using a liquid chromatography–tandem mass spectrometry (LC–MS/MS) system following protein precipitation with acetonitrile (MeCN). The LC–MS/MS system, equipped with a positive electrospray ionization (ESI) surface, consisted of an API5000 tandem mass spectrometer (AB SCIEX) and a Nexera ultra high-performance liquid chromatograph system (Shimadzu). The multiple reaction monitoring mode was selected and monitored the precursor ion (m/z 532.347) and product ion (m/z 145.042). The cone voltage and collision energy were set to 90 V and 55 V, respectively. The column YMC-Triart C18 (3 µm, 2.1 mm Inner Diameter (I.D.) × 50 mm, YMC) was used and column temperature was maintained at 40 °C for chromatographic separation of analytes. The mobile phases were 0.1% (v/v) formic acid in distilled water (mobile phase A) and MeCN (mobile phase B). The flow rate was 0.75 ml min^{-1}. The gradient condition was 30-65-95-95-30 (% of mobile phase B concentration)/0-0.9-0.91-1.1-1.11-1.5 (min). Pharmacokinetic parameters of S-217622 in plasma were calculated by using WinNonlin (Ver. 8.3, Certara, L.P.) on the basis of a non-compartment analysis with uniform weighting. The concentration of S-217622 at 12 h after single oral administration of S-217622 was simulated using a non-parametric analysis from the mean plasma concentration data after single oral administration of S-217622 at 60 mg kg^{-1}.

Evaluation of therapeutic efficacy of mAbs and antiviral compounds in Syrian hamsters. Five- to six-week-old male Syrian hamsters (Japan SLC) were used in this study. For the evaluation of mAb efficacy in hamsters, under isoflurane anaesthesia, five hamsters per group were inoculated intranasally with 10^3 p.f.u. (in 30 µl) of HP095, BA.1 (NC928) or BA.1.1 (NC929). On Day 1 post-infection, the hamsters were injected intraperitoneally with 1 ml of a mAb preparation (5 mg kg^{-1}). The animals were euthanized on Day 4 post-infection, and the virus titres in the nasal turbinates and lungs were determined using plaque assays on VeroE6/TMPRSS2 cells.

For the evaluation of antiviral compound efficacy in hamsters, under isoflurane anaesthesia, four hamsters per group were inoculated intranasally with 10^3 p.f.u. (in 30 µl) of BA.1 (NC928). At 24 h after inoculation, hamsters were treated with the following antiviral compounds: (1) molnupiravir, 500 mg kg^{-1} (in 1 ml) administered orally twice daily; (2) S-217622, 60 mg kg^{-1} (in 1 ml) administered orally twice daily; or (3) methylcellulose (1 ml) as a control for oral treatment. The animals were euthanized on Day 2, 3 or 4 post-infection, and the virus titres in the nasal turbinates and lungs were determined using plaque assays on VeroE6/TMPRSS2 cells.

For the evaluation of the emergence of antiviral-resistant virus in hamsters, CPA was administered intraperitoneally to hamsters on Day −3 (140 mg kg^{-1}), 1 (100 mg kg^{-1}), 5 (100 mg kg^{-1}) and 9 (100 mg kg^{-1}) relative to infection. Under isoflurane anaesthesia, four hamsters per group were inoculated intranasally with 10^3 p.f.u. (in 30 µl) of BA.1 (NC928) on Day 0. At 24 h after inoculation, the hamsters were treated with the following antiviral compounds for 5 d: (1) molnupiravir, 500 mg kg^{-1} (in 1 ml) administered orally twice daily; (2) S-217622, 60 mg kg^{-1} (in 1 ml) administered orally twice daily; or (3) methylcellulose (1 ml) as a control for oral treatment. The animals were euthanized on Day 7 or 14 post-infection, and the virus titres in the nasal turbinates and lungs were determined using plaque assays on VeroE6/TMPRSS2 cells. Viruses were also isolated from lung homogenates for EC_{50} determination and viral genome analysis.

All experiments with hamsters were performed in accordance with the Science Council of Japan's Guidelines for Proper Conduct of Animal Experiments and the guidelines set by the Institutional Animal Care committee. The protocols were approved by the Animal Experiment Committee of the Institute of Medical Science, the University of Tokyo (approval number PA19-75).

ELISA. ELISA was performed as previously reported[37]. Briefly, 96-well Maxisorp microplates (Nunc) were incubated with the recombinant RBD of the S protein or HexaPro prefusion-stabilized versions of the S ectodomain (S_{6pro})[38] (prototype virus or omicron variant) (50 µl per well at 2 µg ml^{-1}), or with PBS at 4 °C overnight and were then incubated with 5% skim milk in PBS containing 0.05% Tween-20 (PBS-T) for 1 h at room temperature. The microplates were reacted for 1 h at room temperature with hamster serum samples (initially diluted 40-fold) or monoclonal antibodies (1 µg ml^{-1}) in PBS-T containing 5% skim milk and subsequently serially 2-fold diluted, followed by peroxidase-conjugated goat anti-human IgG, Fcγ fragment-specific antibody (Jackson Immuno-Research) for 1 h at room temperature. Then, 1-Step Ultra TMB-Blotting solution (Thermo Fisher) was added to each well, followed by incubation for 3 min at room temperature. The reaction was stopped by the addition of 2 M H_2SO_4 and the optical density at 450 nm (OD_{450}) was immediately measured. The average OD_{450} values of two PBS wells were subtracted from the average OD_{450} values of the two RBD or S_{6pro} wells for background correction. A subtracted OD_{450} value of 0.1 or more was regarded as positive; the minimum dilution to give a positive result was used as the ELISA titre (for hamster serum) or the minimum concentration to bind S protein (for monoclonal antibodies).

FRNT. Neutralization activities of SARS-CoV-2 were determined using a focus reduction neutralization assay as previously described[14,39]. Serial dilutions of monoclonal antibodies (starting concentration, 50,000 ng ml^{-1}) were mixed with 1,000 focus-forming units of virus per well and incubated for 1 h at 37 °C. The antibody–virus mixture was inoculated on VeroE6/TMPRSS2 cells in 96-well plates in duplicate and incubated for 1 h at 37 °C. An equal volume of 1.2% Avicel RC-581 (DuPont Nutrition) in culture medium was added to each well. The cells were incubated for 24 h at 37 °C and then fixed with formalin. After the formalin was removed, the cells were immunostained with a mouse monoclonal antibody against SARS-CoV-1/2 nucleoprotein (clone 1C7C7, Sigma-Aldrich), followed by a horseradish peroxidase-labelled goat anti-mouse immunoglobulin (SeraCare Life Sciences). The infected cells were stained with TrueBlue Substrate (SeraCare Life Sciences) and then washed with distilled water. After cell drying, the focus numbers were quantified using an ImmunoSpot S6 Analyzer, ImmunoCapture software and BioSpot software (Cellular Technology). The results are expressed as $FRNT_{50}$ values, which were calculated using GraphPad Prism software.

Determination of EC_{50} values. VeroE6/TMPRSS2 cells were seeded in 96-well plates 1 d before infection and incubated at a multiplicity of infection of 0.01 with SARS-CoV-2 at 37 °C for 1 h. The inocula were then replaced with MEM containing 5% fetal calf serum and serially diluted EIDD-1931 (the active form of molnupiravir) or S-217622, and the cells were incubated at 37 °C with 5% CO_2 for 3 d to observe cytopathic effects (CPE). The EC_{50} was determined using the Spearman–Karber formula[40] on the basis of the appearance of visually detectable CPE in quadruplicate experiments.

Whole-genome sequencing. Viral RNA was extracted using a QIAamp viral RNA mini kit (QIAGEN). The whole genome of SARS-CoV-2 was amplified using a modified ARTIC network protocol as described previously[41]. Briefly, viral complementary DNA was synthesized from the extracted RNA using a LunarScript RT SuperMix kit (New England BioLabs). The DNA was amplified by performing a multiplexed PCR in two pools using the ARTIC-N1 primers v5 and the Q5 Hot Start DNA polymerase (New England BioLabs). The DNA libraries for Illumina NGS were prepared from pooled amplicons using a QIAseq FX DNA library kit (QIAGEN) and were then analysed using the iSeq 100 System (Illumina). To determine the sequence of hCoV-19/Japan/NC929-1N/2021 (Omicron; NC929), the reads were assembled using the CLC Genomics Workbench (version 21, Qiagen), with the Wuhan/Hu-1/2019 sequence (GenBank accession no. MN908947) as a reference. The sequence of NC929 was deposited in the Global Initiative on Sharing All Influenza Data (GISAID) database with accession ID: EPI_ISL_7890636. For the analysis of the viral genomes isolated from the lungs of hamsters treated with antiviral compounds, the reads were assembled using the CLC Genomics Workbench (version 22, Qiagen), with the NC928 sequence (GISAID accession no. EPI_ISL_7507055) as a reference. Amino acid mutations detected at a frequency of ≥10% are listed.

Statistical analysis. GraphPad Prism software was used to analyse all data. We compared virus titres in hamster organs with the control using a one-way analysis of variance (ANOVA) followed by Dunnett's multiple comparisons test, or the Kruskal-Wallis test followed by Dunn's test with multiple comparisons. Differences between groups were considered significant for $P < 0.05$.

Reagent availability. All reagents described in this paper are available through Material Transfer Agreements.

Reporting summary. Further information on research design is available in the Nature Research Reporting Summary linked to this article.

Data availability

All data supporting the findings of this study are available in the paper. There are no restrictions in obtaining access to the primary data. The sequence of hCoV-19/Japan/NC929-1N/2021 (Omicron BA.1.1; NC929) was deposited in the Global Initiative on Sharing All Influenza Data (GISAID) database with accession ID: EPI_ISL_7890636. Source data are provided with this paper.

Code availability

No code was used in the course of the data acquisition or analysis.

Received: 7 January 2022; Accepted: 1 June 2022;
Published online: 15 June 2022

References

1. Walls, A. C. et al. Structure, function, and antigenicity of the SARS-CoV-2 spike glycoprotein. *Cell* **181**, 281–292.e6 (2020).
2. Planas, D. et al. Considerable escape of SARS-CoV-2 Omicron to antibody neutralization. *Nature* https://doi.org/10.1038/s41586-021-04389-z (2022).
3. Cameroni, E. et al. Broadly neutralizing antibodies overcome SARS-CoV-2 Omicron antigenic shift. *Nature* https://doi.org/10.1038/s41586-021-04386-2 (2022).
4. Cao, Y. et al. Omicron escapes the majority of existing SARS-CoV-2 neutralizing antibodies. *Nature* https://doi.org/10.1038/s41586-021-04385-3 (2022).
5. Carreño, J. M. et al. Activity of convalescent and vaccine serum against SARS-CoV-2 Omicron. *Nature* https://doi.org/10.1038/s41586-022-04399-5 (2022).
6. Liu, L. et al. Striking antibody evasion manifested by the omicron variant of SARS-CoV-2. *Nature* https://doi.org/10.1038/s41586-021-04388-0 (2022).
7. Imai, M. et al. Syrian hamsters as a small animal model for SARS-CoV-2 infection and countermeasure development. *Proc. Natl Acad. Sci. USA* **117**, 16587–16595 (2020).
8. Sia, S. F. et al. Pathogenesis and transmission of SARS-CoV-2 in golden hamsters. *Nature* **583**, 834–838 (2020).
9. Chan, J. F. et al. Simulation of the clinical and pathological manifestations of coronavirus disease 2019 (COVID-19) in a golden Syrian hamster model: implications for disease pathogenesis and transmissibility. *Clin. Infect. Dis.* **71**, 2428–2446 (2020).
10. Zalevsky, J. et al. Enhanced antibody half-life improves in vivo activity. *Nat. Biotechnol.* **28**, 157–159 (2010).
11. Dall'Acqua, W. F. et al. Increasing the affinity of a human IgG1 for the neonatal Fc receptor: biological consequences. *J. Immunol.* **169**, 5171–5180 (2002).
12. Oganesyan, V., Gao, C., Shirinian, L., Wu, H. & Dall'Acqua, W. F. Structural characterization of a human Fc fragment engineered for lack of effector functions. *Acta Crystallogr. D* **64**, 700–704 (2008).
13. Corti, D., Purcell, L. A., Snell, G. & Veesler, D. Tackling COVID-19 with neutralizing monoclonal antibodies. *Cell* **184**, 3086–3108 (2021).
14. Takashita, E. et al. Efficacy of antibodies and antivirals against a SARS-CoV-2 Omicron variant. *N. Engl. J. Med.* **386**, 995–998 (2022).
15. Baum, A. et al. Antibody cocktail to SARS-CoV-2 spike protein prevents rapid mutational escape seen with individual antibodies. *Science* **369**, 1014–1018 (2020).
16. Zost, S. J. et al. Potently neutralizing and protective human antibodies against SARS-CoV-2. *Nature* **584**, 443–449 (2020).
17. Chen, R. E. et al. In vivo monoclonal antibody efficacy against SARS-CoV-2 variant strains. *Nature* **596**, 103–108 (2021).
18. Barnes, C. O. et al. SARS-CoV-2 neutralizing antibody structures inform therapeutic strategies. *Nature* **588**, 682–687 (2020).
19. Dong, J. et al. Genetic and structural basis for SARS-CoV-2 variant neutralization by a two-antibody cocktail. *Nat. Microbiol.* **6**, 1233–1244 (2021).
20. Greaney, A. J. et al. Mapping mutations to the SARS-CoV-2 RBD that escape binding by different classes of antibodies. *Nat. Commun.* **12**, 4196 (2021).
21. Garcia-Beltran, W. F. et al. mRNA-based COVID-19 vaccine boosters induce neutralizing immunity against SARS-CoV-2 Omicron variant. *Cell* https://doi.org/10.1016/j.cell.2021.12.033 (2022).
22. Wahl, A. et al. SARS-CoV-2 infection is effectively treated and prevented by EIDD-2801. *Nature* **591**, 451–457 (2021).
23. Bowden, R. A. Respiratory virus infections after marrow transplant: the Fred Hutchinson Cancer Research Center experience. *Am. J. Med* **102**, 27–30 (1997).
24. Englund, J. A. et al. Common emergence of amantadine- and rimantadine-resistant influenza A viruses in symptomatic immunocompromised adults. *Clin. Infect. Dis.* **26**, 1418–1424 (1998).
25. Ison, M. G., Gubareva, L. V., Atmar, R. L., Treanor, J. & Hayden, F. G. Recovery of drug-resistant influenza virus from immunocompromised patients: a case series. *J. Infect. Dis.* **193**, 760–764 (2006).
26. Brocato, R. L. et al. Protective efficacy of a SARS-CoV-2 DNA vaccine in wild-type and immunosuppressed Syrian hamsters. *NPJ Vaccines* **6**, 16 (2021).
27. Kabinger, F. et al. Mechanism of molnupiravir-induced SARS-CoV-2 mutagenesis. *Nat. Struct. Mol. Biol.* **28**, 740–746 (2021).
28. Lempp, F. A. et al. Lectins enhance SARS-CoV-2 infection and influence neutralizing antibodies. *Nature* **598**, 342–347 (2021).
29. Winkler, E. S. et al. Human neutralizing antibodies against SARS-CoV-2 require intact Fc effector functions for optimal therapeutic protection. *Cell* **184**, 1804–1820.e16 (2021).
30. Halfmann, P. J. et al. SARS-CoV-2 Omicron virus causes attenuated disease in mice and hamsters. *Nature* **603**, 687–692 (2022).
31. Meng, B. et al. Altered TMPRSS2 usage by SARS-CoV-2 Omicron impacts infectivity and fusogenicity. *Nature* **603**, 706–714 (2022).
32. Ferren, M. et al. Hamster organotypic modeling of SARS-CoV-2 lung and brainstem infection. *Nat. Commun.* **12**, 5809 (2021).
33. Tomris, I. et al. Distinct spatial arrangements of ACE2 and TMPRSS2 expression in Syrian hamster lung lobes dictates SARS-CoV-2 infection patterns. *PLoS Pathog.* **18**, e1010340 (2022).
34. Matsuyama, S. et al. Enhanced isolation of SARS-CoV-2 by TMPRSS2-expressing cells. *Proc. Natl Acad. Sci. USA* **117**, 7001–7003 (2020).
35. Imai, M. et al. Characterization of a new SARS-CoV-2 variant that emerged in Brazil. *Proc. Natl Acad. Sci. USA* https://doi.org/10.1073/pnas.2106535118 (2021).
36. Yasuhara, A. et al. Antigenic drift originating from changes to the lateral surface of the neuraminidase head of influenza A virus. *Nat. Microbiol.* **4**, 1024–1034 (2019).
37. Yamayoshi, S. et al. Antibody titers against SARS-CoV-2 decline, but do not disappear for several months. *EClinicalMedicine* **32**, 100734 (2021).
38. Hsieh, C. L. et al. Structure-based design of prefusion-stabilized SARS-CoV-2 spikes. *Science* **369**, 1501–1505 (2020).
39. Vanderheiden, A. et al. Development of a rapid focus reduction neutralization test assay for measuring SARS-CoV-2 neutralizing antibodies. *Curr. Protoc. Immunol.* **131**, e116 (2020).
40. Ramakrishnan, M. A. Determination of 50% endpoint titer using a simple formula. *World J. Virol.* **5**, 85–86 (2016).
41. Uraki, R. et al. Characterization and antiviral susceptibility of SARS-CoV-2 Omicron/BA.2. *Nature* https://doi.org/10.1038/s41586-022-04856-1 (2022).

Acknowledgements

We thank Shionogi Co., Ltd. for providing S-217622 and its pharmacokinetic data in hamsters; S. Watson for scientific editing; and K. Yokota for technical assistance. This work was supported by a Research Program on Emerging and Re-emerging Infectious Diseases (JP20fk0108412, JP21fk0108615 and JP20fk0108472), a Project Promoting Support for Drug Discovery (JP20nk0101632), the Japan Program for Infectious Diseases Research and Infrastructure (JP22wm0125002) from the Japan Agency for Medical Research and Development, the National Institutes of Allergy and Infectious Diseases Center for Research on Influenza Pathogenesis (HHSN272201400008C), and the Center for Research on Influenza Pathogenesis and Transmission (CRIPT) (75N93021C00014).

Author contributions

R.U., M.K. and M. Imai performed the in vivo experiments. M.K., S.Y., M. Ito, E.T., M.U., Y.F., A.Y., K.I.-H. and Y.S.-T. performed the in vitro experiments. S.Y. and S.F. performed deep sequencing analysis and interpretation. R.U., M.K., M. Imai, S.Y., S.W., H.H. and Y.K. obtained funding, conceived the study and supervised the research. R.U., M. Imai and Y.K. wrote the initial draft, with all other authors providing editorial comments.

Competing interests

Y.K. has received unrelated funding support from Daiichi Sankyo Pharmaceutical, Toyama Chemical, Tauns Laboratories, Inc., Shionogi & Co. LTD, Otsuka Pharmaceutical, KM Biologics, Kyoritsu Seiyaku, Shinya Corporation and Fuji Rebio. All other authors declare no competing interests.

Additional information

Extended data is available for this paper at https://doi.org/10.1038/s41564-022-01170-4.

Supplementary information The online version contains supplementary material available at https://doi.org/10.1038/s41564-022-01170-4.

Correspondence and requests for materials should be addressed to Yoshihiro Kawaoka.

Peer review information *Nature Microbiology* thanks Robert Garry, Stanley Perlman and the other, anonymous, reviewer(s) for their contribution to the peer review of this work.

Reprints and permissions information is available at www.nature.com/reprints.

Publisher's note Springer Nature remains neutral with regard to jurisdictional claims in published maps and institutional affiliations.

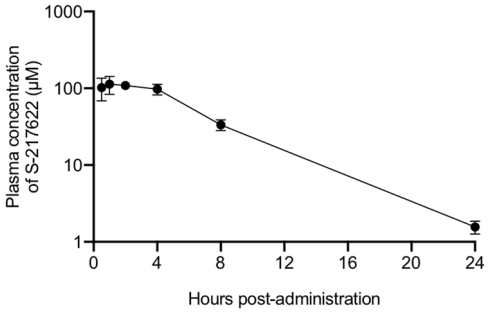

Extended Data Fig. 1 | Plasma concentration profile of S-217622 after single oral administration to hamsters at 60 mg/kg. S-217622 was orally administered to Syrian hamsters at 60 mg/kg under non-fasted conditions. Blood samples (0.1 mL) were collected at 0.5, 1, 2, 4, 8, and 24 h after dosing and the plasma concentrations of S-217622 were determined. Data are expressed as the mean ± SD ($n = 4$/group).

nature portfolio

Corresponding author(s): Yoshihiro Kawaoka

Last updated by author(s): May 18, 2022

Reporting Summary

Nature Portfolio wishes to improve the reproducibility of the work that we publish. This form provides structure for consistency and transparency in reporting. For further information on Nature Portfolio policies, see our Editorial Policies and the Editorial Policy Checklist.

Statistics

For all statistical analyses, confirm that the following items are present in the figure legend, table legend, main text, or Methods section.

n/a	Confirmed	
☐	☒	The exact sample size (*n*) for each experimental group/condition, given as a discrete number and unit of measurement
☐	☒	A statement on whether measurements were taken from distinct samples or whether the same sample was measured repeatedly
☐	☒	The statistical test(s) used AND whether they are one- or two-sided *Only common tests should be described solely by name; describe more complex techniques in the Methods section.*
☒	☐	A description of all covariates tested
☐	☒	A description of any assumptions or corrections, such as tests of normality and adjustment for multiple comparisons
☐	☒	A full description of the statistical parameters including central tendency (e.g. means) or other basic estimates (e.g. regression coefficient) AND variation (e.g. standard deviation) or associated estimates of uncertainty (e.g. confidence intervals)
☐	☒	For null hypothesis testing, the test statistic (e.g. *F*, *t*, *r*) with confidence intervals, effect sizes, degrees of freedom and *P* value noted *Give P values as exact values whenever suitable.*
☒	☐	For Bayesian analysis, information on the choice of priors and Markov chain Monte Carlo settings
☒	☐	For hierarchical and complex designs, identification of the appropriate level for tests and full reporting of outcomes
☒	☐	Estimates of effect sizes (e.g. Cohen's *d*, Pearson's *r*), indicating how they were calculated

Our web collection on statistics for biologists contains articles on many of the points above.

Software and code

Policy information about availability of computer code

Data collection	iSeq 100 System (Illumina) ImmunoSpot S6 Analyzer (Cellular Technology) ImmunoCapture software (Cellular Technology) BioSpot software (Cellular Technology)
Data analysis	Prism 8.0 was used for the statistical analysis.

For manuscripts utilizing custom algorithms or software that are central to the research but not yet described in published literature, software must be made available to editors and reviewers. We strongly encourage code deposition in a community repository (e.g. GitHub). See the Nature Portfolio guidelines for submitting code & software for further information.

Data

Policy information about availability of data

All manuscripts must include a data availability statement. This statement should provide the following information, where applicable:

- Accession codes, unique identifiers, or web links for publicly available datasets
- A description of any restrictions on data availability
- For clinical datasets or third party data, please ensure that the statement adheres to our policy

All data supporting the findings of this study are available within the paper in the Source Data. There are no restrictions to obtaining access to the primary data. All databases/datasets used in this study are available from GISAID database (https://www.gisaid.org), Genbank database (https://www.ncbi.nlm.nih.gov/genbank/), or UniprotKB database (https://www.uniprot.org/). The sequence of hCoV-19/Japan/NC929-1N/2021 (Omicron/BA.1; NC929) is available at GISAID database with Accession ID: EPI_ISL_7890636.

Field-specific reporting

Please select the one below that is the best fit for your research. If you are not sure, read the appropriate sections before making your selection.

☒ Life sciences ☐ Behavioural & social sciences ☐ Ecological, evolutionary & environmental sciences

For a reference copy of the document with all sections, see nature.com/documents/nr-reporting-summary-flat.pdf

Life sciences study design

All studies must disclose on these points even when the disclosure is negative.

Sample size	No sample-size calculations were performed. No statistical method was used to determine sample size. Hamster experiments were performed with at least n = 3 per group. All sample sizes were chosen based on standard practices in the field.
Data exclusions	For antibody-transfer experiments, data were only excluded when the antibody levels in plasma were low (<640) after transfer of human mAbs because low antibody levels indicate the failed passive transfer of mAbs.
Replication	All experiments with multiple biological replicates are indicated in the figure legends.
Randomization	No method of randomization was used to determine how the animals were allocated to the experimental groups and processed in this study. However, covariates including sex and age were identical in groups.
Blinding	No blinding was carried out due to the limited number of staff available to conduct these studies.

Reporting for specific materials, systems and methods

We require information from authors about some types of materials, experimental systems and methods used in many studies. Here, indicate whether each material, system or method listed is relevant to your study. If you are not sure if a list item applies to your research, read the appropriate section before selecting a response.

Materials & experimental systems

n/a	Involved in the study
☐	☒ Antibodies
☐	☒ Eukaryotic cell lines
☒	☐ Palaeontology and archaeology
☐	☒ Animals and other organisms
☒	☐ Human research participants
☒	☐ Clinical data
☒	☐ Dual use research of concern

Methods

n/a	Involved in the study
☒	☐ ChIP-seq
☒	☐ Flow cytometry
☒	☐ MRI-based neuroimaging

Antibodies

Antibodies used	Amino acid sequences for the variable region of the heavy and light chains of the following human monoclonal antibodies against the S protein were used for gene synthesis: clones tixagevimab (COV2-2196/AZD8895; GenBank accession numbers QLI33947 and QLI33948), casirivimab (REGN10933; PDB accession numbers 6XDG_B and 6XDG_D), cilgavimab (COV2-2130/AZD1061; GenBank accession numbers QKY76296 and QKY75909), imdevimab (REGN10987; PDB accession numbers 6XDG_A and 6XDG_A), and S309 (PDB accession numbers 6WS6_A and 6WS6_F). An artificial signal sequence and the constant gamma heavy (IgG1, UniProtKB/Swiss-Prot accession number P01857) and kappa (UniProtKB/Swiss-Prot accession number P01834) or lambda (UniProtKB/Swiss-Prot accession number P0DOY2) light chain coding sequences were added before and after each variable region. Codon usage was optimized for expression in CHO cells. The synthesized genes were cloned into a plasmid for protein expression and transfected into CHO cells. Cell culture media were harvested after incubation for 10–14 days at 37 °C. A human monoclonal antibody (1430E3/9) against the hemagglutinin of influenza B virus was previously identified in our group and cloned into the expression vector Mammalian Power Express System (TOYOBO) and was transiently expressed by Expi293 cells. Monoclonal antibodies were purified by using MabSelect SuRe LX (Cytiva) or a protein A column. Purity was confirmed by SDS-PAGE and/or HPLC before use. Peroxidase-conjugated goat anti-human IgG, Fcγ Fragment specific antibody (Cat# 109-035-098, Jackson Immuno-Research) was used as the secondary antibody in the ELISA. A mouse monoclonal antibody against SARS-CoV-1/2 nucleoprotein [clone 1C7C7 (Sigma-Aldrich)] and a horseradish peroxidase-labeled goat anti-mouse immunoglobulin (SeraCare Life Sciences) were used for the focus reduction neutralization test. A peroxidase-conjugated goat anti-human IgG, Fcγ Fragment specific antibody (Jackson Immuno-Research) was used for Enzyme-linked immunosorbent assays (ELISAs).
Validation	The therapeutic monoclonal antibodies were validated in previous publications: Takashita, E. et al. Efficacy of Antibodies and Antiviral Drugs against Covid-19 Omicron Variant. N Engl J Med, doi:10.1056/

NEJMc2119407 (2022)

The human monoclonal antibody (1430E3/9) against the hemagglutinin of influenza B virus was validated in a previous publication: Yasuhara, A. et al. Antigenic drift originating from changes to the lateral surface of the neuraminidase head of influenza A virus. Nat Microbiol 4, 1024-1034, doi:10.1038/s41564-019-0401-1 (2019).

The mouse monoclonal antibody against SARS-CoV-1/2 nucleoprotein [clone 1C7C7 (Sigma-Aldrich)], the horseradish peroxidase-labeled goat anti-mouse immunoglobulin (SeraCare Life Sciences), and the peroxidase-conjugated goat anti-human IgG, Fcγ Fragment specific antibody (Jackson Immuno-Research) were validated in a previous publication:
Takashita, E. et al. Efficacy of Antibodies and Antiviral Drugs against Covid-19 Omicron Variant. N Engl J Med, doi:10.1056/NEJMc2119407 (2022).

Eukaryotic cell lines

Policy information about cell lines

Cell line source(s)	VeroE6/TMPRSS2 cells (available at Japanese Collection of Research Bioresources Cell Bank, JCRB 1819); Expi293F cells (available at Thermo Fisher Scientific); CHO cells (available at GenScript)
Authentication	VeroE6/TMPRSS2, Expi293F, and CHO cells were assumed to have been authenticated by the cell bank or manufacturers. No further authentication was performed by the authors.
Mycoplasma contamination	All cell lines are routinely tested each month and were negative for mycoplasma.
Commonly misidentified lines (See ICLAC register)	No commonly misidentified lines were used in this study.

Animals and other organisms

Policy information about studies involving animals; ARRIVE guidelines recommended for reporting animal research

Laboratory animals	Male Syrian hamsters (5- to 6-week-old) were obtained from Japan SLC Inc., Shizuoka, Japan.
Wild animals	No wild animals were used in this study.
Field-collected samples	This study did not involve samples collected from the field.
Ethics oversight	All experiments with hamsters were performed in accordance with the Science Council of Japan's Guidelines for Proper Conduct of Animal Experiments and the guidelines set by the Institutional Animal Care. The protocols were approved by the Animal Experiment Committee of the Institute of Medical Science, the University of Tokyo (approval number PA19-75).

Note that full information on the approval of the study protocol must also be provided in the manuscript.